

## Microstructure Evolution of A356 Alloy Under Modification by Antimony

Abdelfattah. A. Khalil

Materials Science Department, Faculty of engineering, Omer Al Muktar university, ALBEIDA, LIBYA.

\*Corresponding author: E-mail addresses: [abdelfattah.ahmed@omu.edu.ly](mailto:abdelfattah.ahmed@omu.edu.ly)

Volume: 4

Issue: 1

Page Number: 15 - 25

### Keywords:

Aluminium alloy A356, Modifier Sb,  
Optical microscopy, SEM, EDS.

### ABSTRACT

The effects of antimony (Sb) addition on the microstructure properties of Solidified A356 alloy were investigated. A356–X wt. %Sb (X = 0, 0.1, 0.2 and 0.3) alloys were fabricated using by the permanent mold process. Two different approaches to modification by solidification process have been pursued physically induced and chemically stimulated. The physical relies mainly on the use of external field, such as ultrasonic vibration, while the chemical rout depends primarily on addition of element, which is the subject of this research work. Antimony was used to modify the microstructure of A356 alloy. The effect of addition level of antimony on the solidification of the A356 alloy was investigated and the obtained samples were characterized by optical microscopy, scanning electron microscopy (SEM) and X-ray analysis (EDS). The results displayed that: 1) both the dendritic  $\alpha$ -Al solid solution and eutectic silicon were significantly modified; 2) the dendritic primary aluminium became globular, and the plate-like or big spherical eutectic silicon turned into fibrous shape and small spheres during the solidification process. The mechanism of the microstructure evolution under inoculated by Sb element was also preliminarily discussed.

Copyright: © 2024 by the authors. Licensee The Derna Academy for Applied Science (DAJAS). This article is an open access article distributed under the terms and conditions of the Creative Commons Attribution (CC BY) License (<https://creativecommons.org/licenses/by/4.0/>).



Received: 15\05\2025

Accepted: 30\06\2025

Published: 02\07\2025

DOI: <https://doi.org/10.71147/pj9gsv72>



### 1. INTRODUCTION

Water-cooled cylinder blocks, automotive gearbox cases, aircraft fittings and control parts, and other applications requiring excellent castability, good weldability, pressure tightness, and strong corrosion resistance are all made of the common alloy A356 (Zhu M. et, al 2009). Modification of the eutectic silicon from an acicular to a fine fibrous structure can be achieved in two different ways chemical modification (addition of certain elements) and quench modification (rapid cooling rate). Chemical modification is known to occur in a number of elements; the most widely used elements in modern industry are Sr, Na, and Sb. Modification by Sr and Na changes the morphology of eutectic silicon into fine fibrous forms, whereas Sb causes a refinement in the plate like silicon structure.

Additions of other alkali, alkaline earth and rare-earth metals have also been reported to cause modification (Yu-Chou, et. al 2009, Hao Dong, et.al, 2020, Muhammad, et. al 2024). It has been found that Sb can effectively refine the Al–Si eutectic structure at casting properties. Sb in the form of Al–Sb master alloys is extensively used as an alternative to Na or Sr in the production of Al–Si alloys by the permanent mold process. In the industrial practice, Sb is often added to the Al–Si melts in the form of Al–Sb master alloy. It has been also reported that Sb results in fine lamellar morphology of eutectic silicon (Karakosea, et.al, 2009, Peng Tang. et. al, 2023). Recently work has indicated that three eutectic nucleation and growth modes are possible in gradient; (Yu-Chou, et. al 2009). Nucleation and growth on the primary aluminium dendrites and , (Hao Dong, et.al, 2020). Independent heterogeneous nucleation of eutectic grains in interdendritic spaces. The authors have recently proposed for causing the observed transition in eutectic nucleation and growth (Kazuhiro. et.al 2001). Modification of aluminum alloys is process by which the melt is deliberately modified by various elements in order to influence the mechanism of eutectic solidification. Modification changes the morphology and size of crystals of silicon (in the case of Silumin), resulting in a notable improvement in mechanical characteristics above those of unaltered alloys. Large silicon crystals reduce the Al-Si alloy's strength characteristics while significantly improving its mechanical qualities as compared to unmodified alloys. The strength of Al-Si alloys is reduced by large silicon crystals. Strength and plastic properties of the modified alloys are therefore higher in comparison to unmodified alloys. Changing the structure may also affect the machinability of the modified alloy. Strength and plastic properties of the modified alloys are therefore higher in comparison to unmodified alloys. Modification is meaningful only for aluminum alloys with a silicon content of more than 5% (Pavel Krausl. et.a, 2008).

## 2. EXPIRMENTS

### Materials

The commercial aluminum-silicon based alloy A356 is the material of interest in this study. Table 1 displays its chemical composition, which was supplied by the source "ASTM."

Table 1. Chemical composition of A356 “ASTM”.

Parameter	Values
Min	6.5%Si, 0.20%Mg, Al balance.
Max	7.5%Si, 0.6%Fe, 0.35%Mn, 0.25%Cu, 0.45%Mg 0.35%Zn, 0.25%Ti, other 0.15%, Al balance

Aluminum Company of Egypt supplied this alloy in the ingot form A356, which was subsequently chemically analyzed (real analysis) using the optical immersion procedure. The outcome is displayed in Table 2.

Table 2. Chemical composition of A356.

Values
7.36%Si, 0.15%Fe, 0.00129%Mn, 0.0462%Cu, 0.329%Mg 0.00229%Zn, 0.136%Ti, other 0.012%, Al balance

The equilibrium eutectic constitution is around 12.6 weight percent silicon, according to the aluminum-silicon phase diagram. This study's selected aluminum alloy is regarded as a hypoeutectic Al-Si alloy. Its eutectic temperature of 577°C marked the end of solidification, whereas its liquidus temperature began at 614°C. Both the basic fcc aluminum solid solution, which contains 7.36 weight percent silicon, and the eutectic, which contains silicon-enriched aluminum and pure silicon, make up the microstructure (Polmear, 2006).

### Addition of of modifier

In a heat-resistant furnace, 1500 grams of A356 alloy were melted using a steel crucible that had been internally coated in graphite. After complete melting of the alloy, the temperature of the molten metal was kept at a temperature of 740 °C± 10 °C, which is higher than its liquidus temperature by about 125 °C to allow the complete dissolution of the silicon particles.

Antimony (Sb) was used in this investigation as a modifier, then treated with addition different amounts of antimony such as 0% , 0.1%, 0.2%, 0.3% respectively. A steel rod covered in graphite was used to physically stir the melt after the modifier was added, and it was kept at 740 °C for five minutes to homogenize it. The temperature during the melting process was measured using a type K thermocouple. Each melt series was preceded and followed by a calibration of the thermocouple.

#### preparations of Permanent mould

The alloy was melted and then poured at room temperature into a permanent cast iron mold. As seen in Figure 1, the permanent mold's dimensions were 200 mm in length and 40 mm in internal diameter.



Fig.1 Used permanent mould.

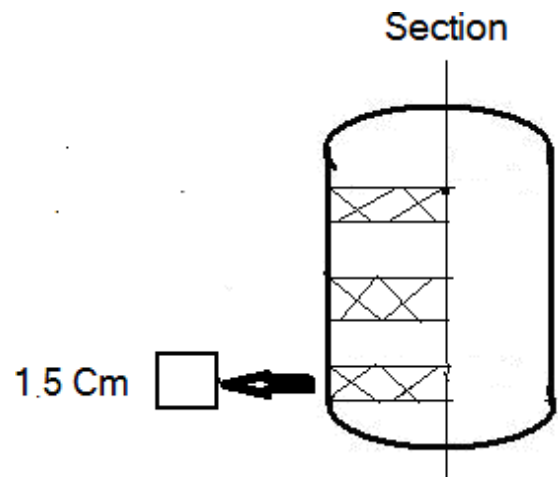


Fig. 2 location of specimens A356

#### Microstructure Analysis

As seen in Fig. 2, metallographic samples were prepared in accordance with established protocols for the development of aluminum alloys and cut from the same location for every experiment, 15 mm from the bottom of the casting. Grain refiners in varying amounts 0%, 0.1%, 0.2%, and 0.3%, respectively were added to the investigated specimens. Sectioning the cylinders parallel to the longitudinal axis of each cast sample allowed for the creation of three specimens for microstructure investigation from a single section; these specimens are positioned 15 mm apart from the bottom of the cast, as illustrated in Fig. 2. Standard metallographic techniques were used to first cut and grind the samples. 240, 320, 400, and 600 grit papers were being used for grinding. Samples were polished using 0.05  $\mu\text{m}$  and 1  $\mu\text{m}$  alumina suspension in water after grinding. Silica suspension was used for the final polishing. Samples were carefully cleaned in between each procedure.

#### Optical microscopy and quantitative characterization

To show the resultant microstructure, samples utilized for optical microscopy characterization were etched using a 0.5% HF solution (Zhongtao et al., 2009). Using the linear intercept approach, the microstructure obtained from polarized light under an optical microscope at 400X is used to measure the grain size, length, and width of both eutectic silicon and  $\alpha$ -aluminum. Image C software is used to process six digital micrographs. The data are averaged over ten readings.

#### Scanning electron microscopic (S.E.M.)

Using a scanning electron microscope (SEM) fitted with an Energy Dispersive X-ray spectroscopy (EDS) analysis system, the composition of the intermetallic phase, eutectic Si morphology, and three-dimensional  $\alpha$ -aluminum phase were examined in the specimens by deep-etched solution. Two deep etching methods were used in this investigation. The initial methods involved immersing the specimens in a 30% NaOH solution in distilled water at 70 °C for three to twenty minutes.(ASM, 2005) In the second, the specimens were submerged for 15 to 20 minutes in a solution containing 15 cm<sup>3</sup> HCL, 10 cm<sup>3</sup> HF, and 90 cm<sup>3</sup> H<sub>2</sub>O (distilled water). They were then submerged for 1 to 2 minutes in water, then for 3 to 5 minutes in alcohol, and finally for 60 minutes in a dryer set at 80 °C (Waly, 1993).



### 3. RESULTS

#### Microstructure of A356

Figure 3 displays typical optical microscopy pictures of the A356 alloy after the addition of the (0, 0.1, 0.2, 0.3) weight percentage Sb element. As can be observed in Fig. 3a, the as-cast A356 alloy is composed of primary  $\alpha$ -Al dendrites and interdendritic needle/plate-like eutectic silicon that distributes randomly when there is no modifier present. But when the antimony element is added, the eutectic silicon needles get smaller and the microstructures transform from coarse dendrites to a tiny microstructure. Fig. 4(a-f) displays the sample's SEM image at various magnifications. The base aluminum alloy A356 exhibits huge, completely dendritic  $\alpha$ -aluminum flakes. As illustrated in Fig., EDS was performed in the SEM to examine the nature and composition of samples that were described by SEM. The three-dimensional SEM morphology of eutectic silicon is depicted in Fig. 5(a, c). The original sample's eutectic silicon phase had a typical coarse plate-like shape. Eutectic silicon phases with a long needle form are seen in the aluminum matrix, according to an EDS study in Figure 4(c,d).

#### The impact of Sb on aluminum alloy A356's microstructure

The microstructure of the A356 alloy inoculated with 0.1% Sb is shown in Fig. 6(a, b, c, d). It is evident that the addition of 0.1% Sb causes the eutectic silicon needles to shrink in size. The outcomes are displayed in table 3.3

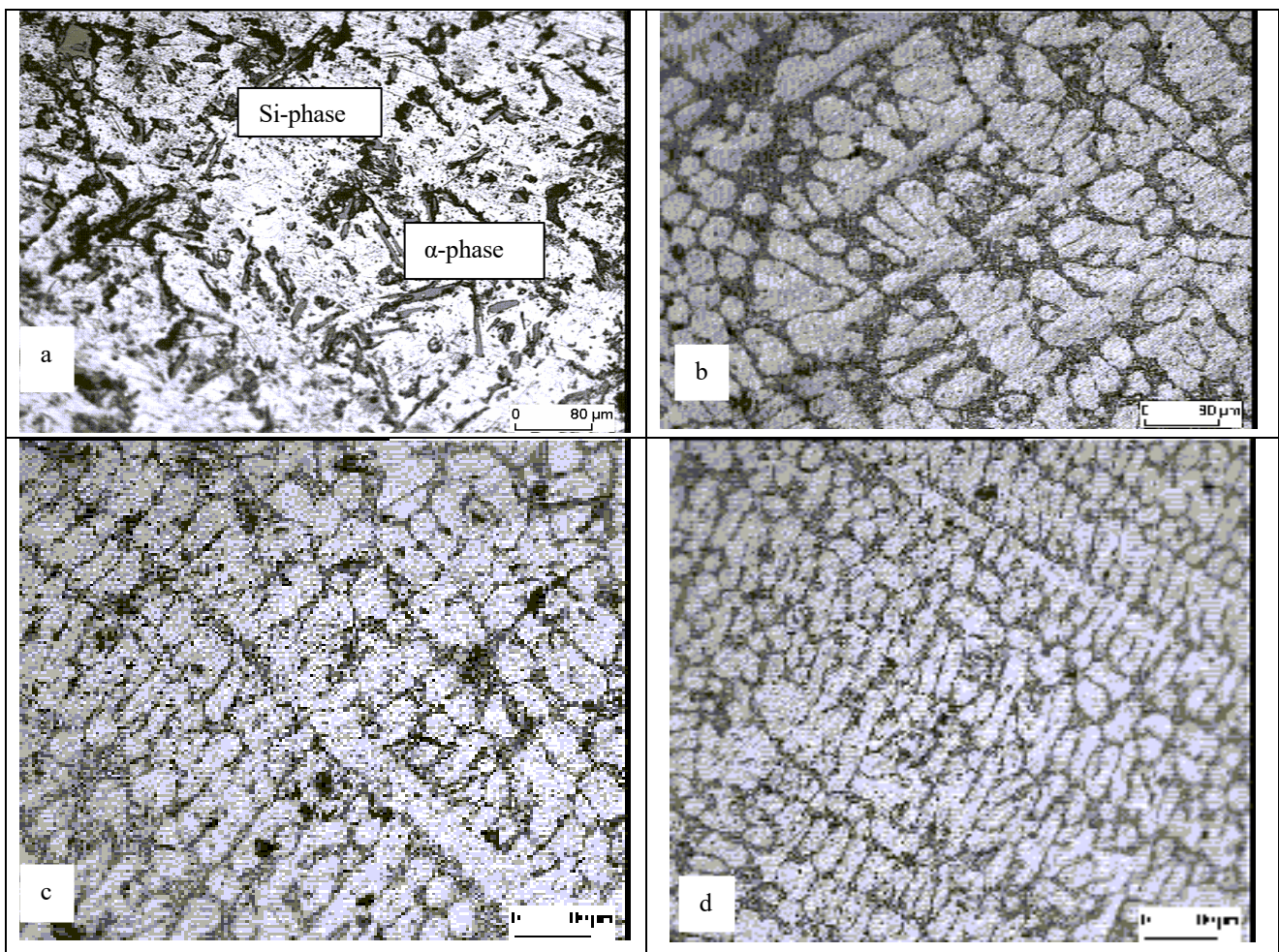


Fig.3 Optical micrograph of A356 modified by a)0 %Sb, b) 0.1 % Sb, c) 0.2 %Sb, d)0.3 Sb.

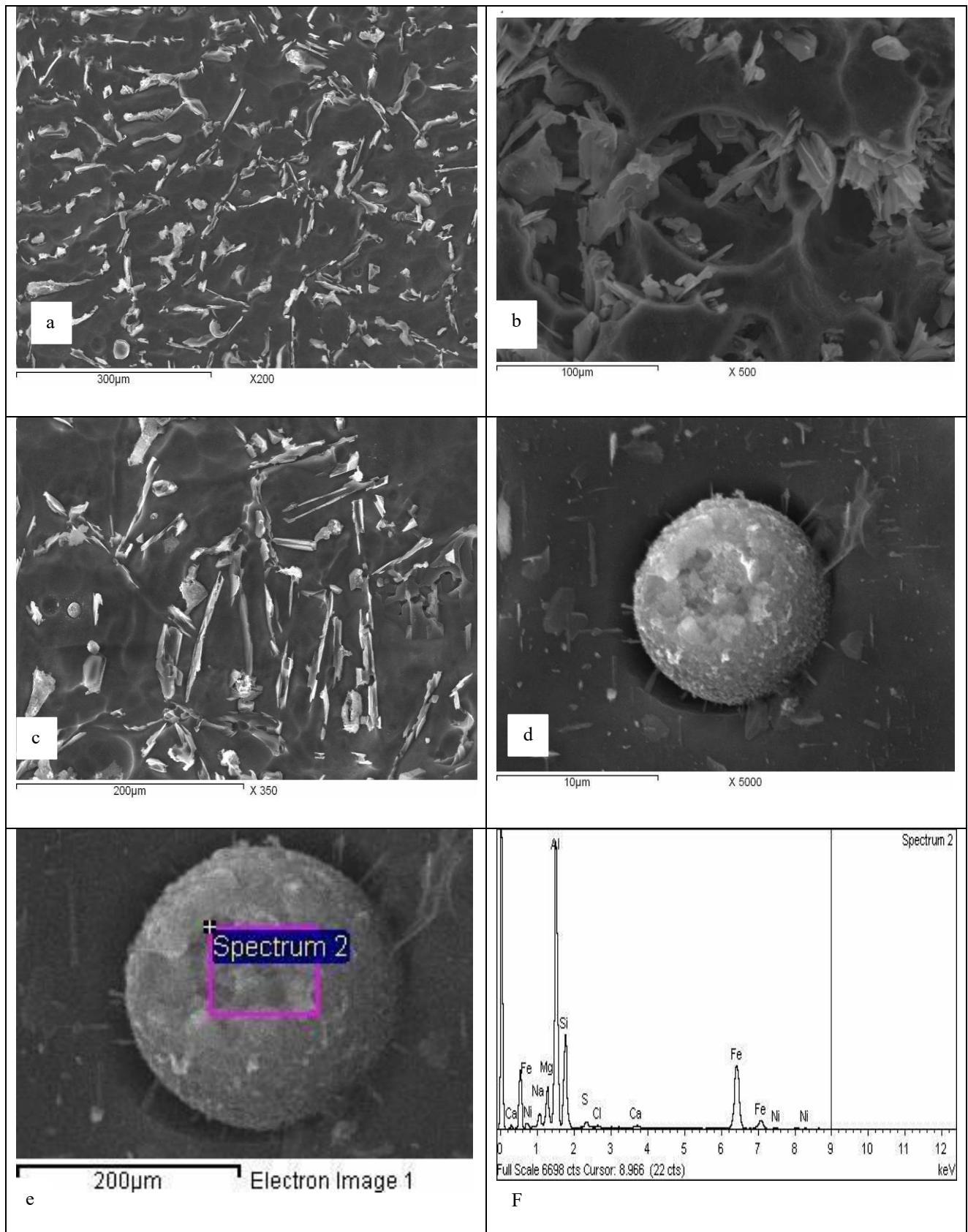


Fig. 4 Intermetallics in alloy A356 were identified using SEM micrographs (a, b, c) and EDS (morphology of intermetallics (d, e, ) (f) composition).



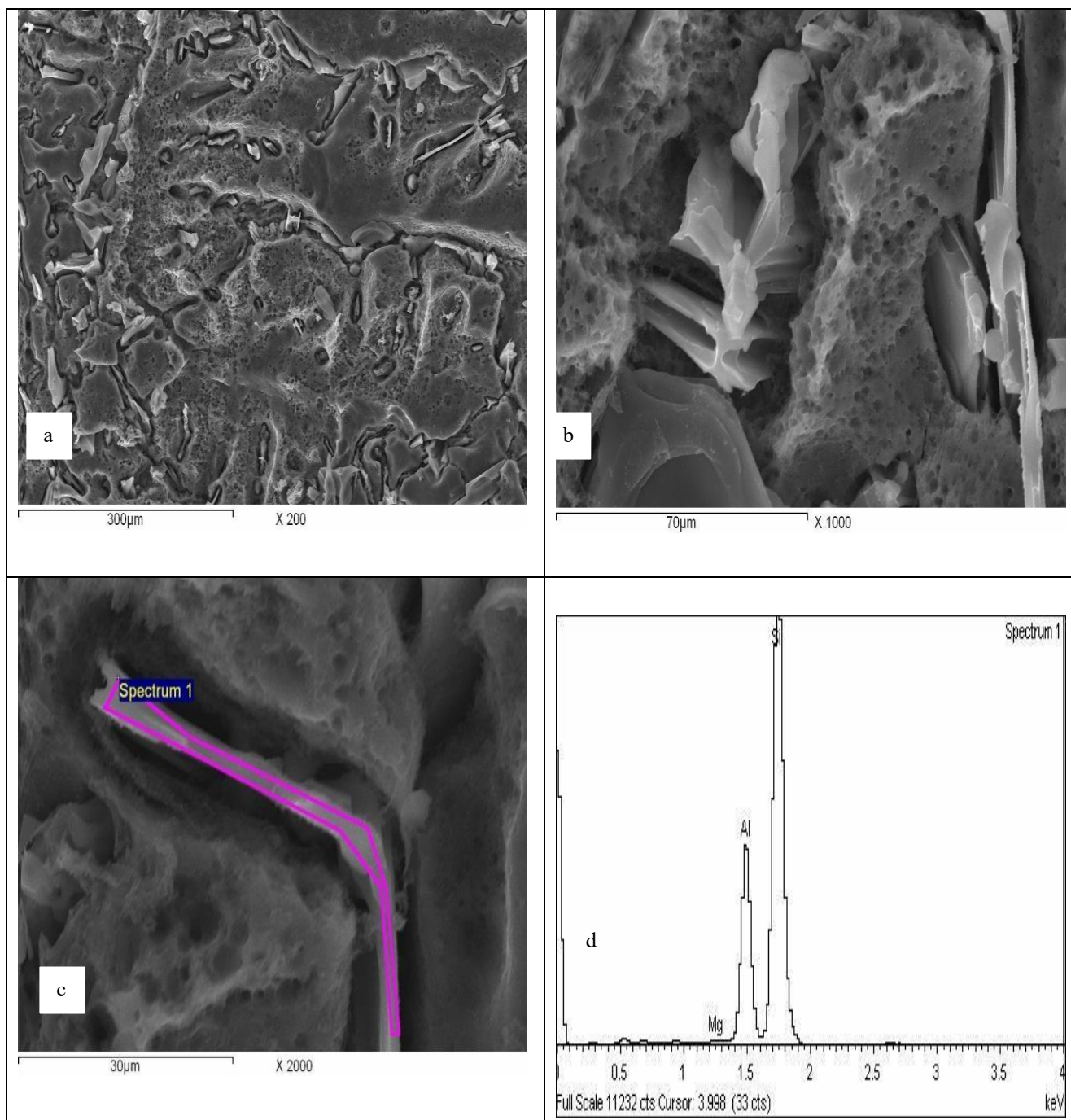


Fig.5 Identification of the silicon phase in experimental alloy A356 using SEM micrographs and EDS (a, b, and c); shape of the silicon phase in base alloy A356 (d); and composition analysis of the silicon phase

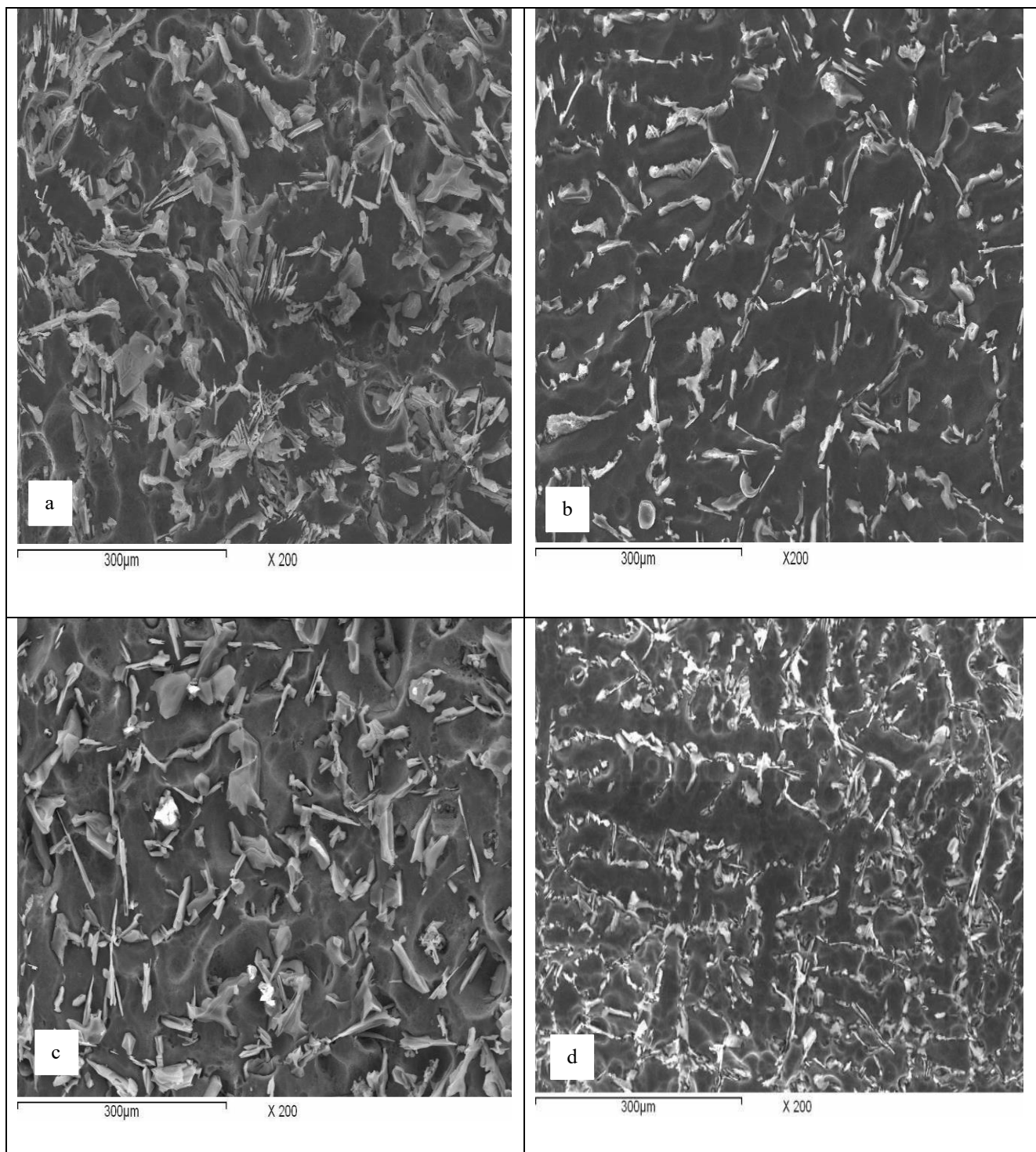


Fig. 6 SEM photomicrographs of the as-cast A356 0 % Sb (a, c), 0.1 Sb % (b, d).

Table 3 Typical grain size of  $\alpha$  - aluminium

Antimony Wt. %	0.1%	0.2%	0.3%
	320 $\mu\text{m}$	300 $\mu\text{m}$	280 $\mu\text{m}$



## 4. DISCUSSION

### Microstructure of A356

As illustrated in Fig. 3(a), the original sample had coarse acicular eutectic silicon scattered among the fully developed primary  $\alpha$ -aluminum dendrites, exhibiting a microstructure of fully dendritic aluminum alloys A356. The eutectic silicon measured approximately 32.3  $\mu\text{m}$  in length and had an average area of 122  $\mu\text{m}^2$  in the interdendritic areas. One branch of a primary  $\alpha$ -aluminum was about 1200  $\mu\text{m}$  in length, as shown in Fig. 3(a), which indicated that the grain size was about a few millimetres as one grain usually contained several arms. The microstructure of hypoeutectic aluminium alloys such as A356, besides a usually coarse and dendritic  $\alpha$ -Al solid solution "white" and Al-Si eutectic, where Si usually assumes a long plate or big rounded shape "dark gray". Several investigations have shown the presence of intermetallic phases that form in the interdendritic and intergranular areas. These include the long, pointed needles of  $\beta$ - $\text{Al}_5\text{FeSi}$  and the eutectic  $\text{Al}_2\text{Cu}$  "Chinese script" shaped  $\alpha$ - $\text{Al}_{15}(\text{Mn},\text{Fe})_3\text{Si}_2$  (Puga et al., 2011). Fig. 4(a,b) displays the sample's SEM image at various magnifications. The base aluminum alloy A356 exhibits huge, completely dendritic  $\alpha$ -aluminum flakes. As seen in Fig. 4(a, b, c, d), EDS was performed in the SEM to examine the nature and content of samples that were described by SEM. At a high magnification of 350, it is evident that the microstructure of the A356 alloy is entirely dendritic for each  $\alpha$ -aluminum, silicon, and other intermetallic phase inside the microstructure, a tiny sphere-shaped intermetallic phase particle is visible. The nature and chemical makeup of the small sphere particle shape are seen in the aluminum alloy A356, according to an EDS study in Fig. 4.(e, f). Instead of silicon or aluminum components, the EDS X-ray examination confirmed that the particles observed in the eutectic zones were primarily intermetallic phases and inclusions. The precipitates present (particles within the A356 alloy) are Na, Ni, Ca, S, and Cl, as indicated in element map Fig. 4.(f). The compound of particles contains the components Al, Si, Fe, and Mg atoms, along with other weakly included elements. In the specific instance of the hypoeutectic alloy A356, aside from the Al-Si eutectic, where Si typically takes on the structure of a huge plate, and the typically coarse and dendritic  $\alpha$ -Al solid solution. Puga et al. (2011) reported that the hypoeutectic  $\text{AlSi}_9\text{Cu}_3$  alloy had the same intermetallic phase as the non-treated aluminum alloys A356, which showed the presence of intermetallic phases such as the eutectic "Chinese script" shaped  $\alpha$ - $\text{Al}_{15}(\text{Mn},\text{Fe})_3\text{Si}_2$  and long and sharp needles of  $\beta$ - $\text{AlSi}_9\text{Cu}_3$  that precipitate in the interdendritic and intergranular regions. This shape not only has a detrimental effect on the mechanical properties of the alloy, but it can also promote shrinking porosity because the platelets physically block the flow of compensatory feeding liquid, so restricting feeding. Aggregation was discovered across the section of the samples Fig. 3(a) and Fig. 4(a) due to the non-uniform distribution of the primary Si phase in the aluminum alloy A356. The original Si phase's forms were primarily blocky crystals or coarse, massive polygons. The main Si phase's corners and edges were visible. The primary Si phase reached a maximum length of 50  $\mu\text{m}$ . The three-dimensional SEM morphology of eutectic silicon is depicted in Fig. 5(b, c). The original sample's eutectic silicon phase had a typical coarse plate-like shape. Eutectic silicon phases with a long needle form are seen in the aluminum matrix, according to an EDS study in Figure 5(c,d). Instead of intermetallic phases or inclusions, the EDS X-ray analysis, which is displayed in Fig. 5(d), confirmed that the needles in the eutectic zones were primarily elemental silicon. As seen in Fig. 5(d), the needle-like compound contains Si, Al, and Mg atoms, although its primary constituents are aluminum and eutectic silicon phase, respectively. It has been documented elsewhere that a needle or long dendritic can grow between the primary aluminum phase, primarily from silicon (Jiana et al., 2006). The eutectic is formed by combining a solid aluminum solution with little more than 1% silicon and practically pure silicon as the second phase. The eutectic composition has been disputed, but recent investigations with high purity binary alloys have shown that it is Al-12.6 Si, with the change occurring at 577.6 °C. The eutectic is a very coarse microstructure formed by the gradual solidification of a pure Al-Si alloy. It is composed of large silicon plates or needles in a continuous aluminum matrix. Figure 4(b). The eutectic itself is made up of several cells that provide the impression that the silicon particles are connected (Polmear, 2006).

### The impact of Sb on the microstructure of Aluminium alloy A356

The as-cast microstructures of A356 alloys with different concentration of Sb ( 0.1%, 0.2%, 0.3%) respectively. Fig. 3(b, c, d) shows the optical photo micrograph of as cast A356 alloy without addition of Sb. The microstructures seen reveal coarse platelets of eutectic silicon and dendrites of  $\alpha$ -Al as shown in Fig. 5(a, b). Figs. 3(b) and 5(c, d) show the microstructure of the 0.1% Sb-inoculated A356 alloy. It is evident that the addition of 0.1% Sb causes the eutectic silicon needles to shrink in size. Additionally, it is clear that eutectic silicon needles get smaller. The microstructure of the A356 alloy inoculated with 0.2% and 0.3% Sb is shown in Fig. 3(c, d). It is clear that adding 0.2% Sb causes the eutectic silicon needles to shrink in size. It is clear that when eutectic silicon needles are inoculated with 0.2% Sb as opposed to 0.1% Sb, their size becomes finer. Similar trend is also shown in Fig. 3 (b,c) for Sb addition levels of 0.2 and 0.3%. However, as seen in Figs. 3(b, c, d) and 5(c, d) correspondingly, the morphology of the eutectic silicon changed from coarse acicular to lamellar or fibrous shape upon the addition of Sb modifiers to the A356 alloy. The majority of the silicon particles were reshaped into rounded shapes in Fig. 5(c) and rods with blunted tips in Fig. 5(c, d).

The coarse type structure changed to a fully modified structure, and the acicular Si phase was totally missing. Additionally, using quantitatively analyzed software and the linear intercept approach, average grain diameters at various Sb element levels were determined; the results are displayed in table 3. Before any modifications were made, the average grain size of A356 was several millimeters.



This outcome is consistent with earlier research (Jiana et al., 2005). As seen in Fig. 3(d), the dendritic structure was fragmented and transformed into a slightly spherical grain structure upon inoculation with the Sb element. According to the table3, the average grain size was roughly 320  $\mu\text{m}$ . The amount of Sb element added may be related to the reduction in grain size. Grain size decreased from 320 to 300  $\mu\text{m}$  when the inclusion of Sb element was increased from 0.1% to 0.2%. The grain size grew to 280  $\mu\text{m}$  when the addition was raised to 0.3%, indicating a notable variation in grain size between the various levels of Sb element alloy that were tested. The impact of different concentrations of Sb modifier on the average grain size of the cast specimens is displayed in Table 3. It is evident that increasing the Sb element in the alloy from 0 to 0.1 weight percent can produce a fine microstructure and an almost noticeable decrease in the average grain size. However, the average grain size decreased when grain refiner (0.2, 0.3 weight percent) was added to the alloy. Grain size has an inverse relationship with the number of solidification nuclei in the liquid alloy that will act during solidification. The more nuclei there are, the more grains will form and the smaller the grain will be, because each grain starts from a single nucleus. Globular grains of primary  $\alpha$ -Al will preferentially form if there are enough nuclei, and dendritic structures may vanish since they won't have space to grow. The addition of the Sb element to the Al-Si alloy results in a fibrous silicon structure and, in certain locations, a lamellar structure that is halfway between acicular and fibrous. A fibrous silicon structure and, in certain places, a lamellar structure that is halfway between acicular and fibrous are the results of adding the Sb element to the Al-Si alloy. Nevertheless, it has been seen that Sb can effectively improve the Al-Si eutectic structure, providing it with better casting properties and a reduced gassing susceptibility. As a result, Sb has been used to create Al-Si alloys instead of Na and Sr. It is well known that Sb works more frequently as a eutectic silicon refining agent in Al-Si alloys and refines the eutectic Si phase at concentrations of 0.05% or higher. Typical quantities in Sb-treated alloys described in the literature range from 0.05% to 0.8%, depending on the nature of the alloy. 0.5% Sb addition enhanced the Al-12Si alloy's microstructure, but 1.0% Sb addition led to the formation of coarse Si particles (Jiana et al., 2006). Conversely, the Sb concentration increases from top to bottom when the melt is stored for an extended period of time. This could be due to the difference in the densities of Sb ( $\sim 6.4 \text{ g/cm}^3$ ) and Al ( $\sim 2.385 \text{ g/cm}^3$ ). Upon maintaining the melt at 720 degrees Celsius (Brandes, 1998), antimony slowly descends to the crucible's bottom. Sb takes a while to fall to the bottom of the melt, based on the data above. Furthermore, a greater degree of addition is seen to increase the urge to settle. The Sb concentration of Al-7Si alloy castings varies from top to bottom, Prasada Rao et al. (2008). During a 5-minute holding time, the Sb concentration decreases from the top to the bottom of the casting at both 0.2 and 0.5 weight percent addition.

#### Proposed mechanism of modification by Sb

As the solidification of A356 liquid continues from 720 °C, the reaction between Al and Sb in the liquid produces AlSb at 657 °C (Prasada Rao et al., 2008). This result suggests that enhanced eutectic silicon refinement is not a result of a higher Sb concentration in liquid A356. However, according to some earlier research, the shift in eutectic silicon in Al-Si-alloys (with trace amounts of Sb) is due to constitutional super cooling. However, these theories failed to explain why eutectic silicon changed more favorably over a longer holding period for a given Sb addition quantity (Qiyang. et. al, 1998). Long-term storage of the Sb-treated Al-7Si alloy has been shown to cause the development of AlSb particles in the casting. These AlSb particles may enhance the modification (refinement) of eutectic silicon in long-holding melts by encouraging the nucleation of Si particles. In the Al-Si eutectic melt, antimony neutralizes phosphorus in a manner similar to that of sodium and strontium. The compound  $\text{Mg}_3\text{Sb}_2$ , which is produced when antimony and magnesium combine, dissolves phosphorus. In the absence of magnesium, aluminum and antimony combine to form AlSb. which has an effect comparable to that of  $\text{Mg}_3\text{Sb}_2$ . In the Al-Si eutectic melt, antimony's activity is irreversible (Khan. et. al, 1994). Upon further cooling, a eutectic reaction occurs, producing Si and  $\alpha$ -Al. These eutectic silicon needles are most likely altered by improved nucleation by liquid-soluble AlSb substrates (produced on prolonged melt holding time). Therefore, the more Sb is added, the more AlSb particles are supplied, which leads to improved modification (refinement) of the eutectic silicon particles in the fully formed A356 alloy. According to a number of researchers, the primary cause of antimony's alteration of Al-Si alloy is the development of the intermetallic phase (AlSb). It enhances the eutectic silicon particles' refinement in their fully solidified state (Uzun et al., 2011, Prasada Rao et al., 2008, Bian et al., 2001).

## 5. CONCLUSION

This study investigates the impact of Sb element addition on the microstructure properties of A356 alloy. The study inspects the microstructural changes, and also talks about the modification mechanism of the base alloy with Sb element addition. The following conclusions can be drawn:

- (1) The dendritic structure of the  $\alpha$ -Al phase was broken up and transformed into a slightly spherical grain structure when Sb was added to A356. Grain size averaged around 320  $\mu\text{m}$ . The addition of the Sb element may be the cause of the grain size decrease. While increase addition of Sb element from 0.1% to 0.3% led to decrease in grain size from 320 to 280  $\mu\text{m}$ . It can be seen that the increase of Sb element from 0 to 0.3 wt. % in the alloy can result in a fine microstructure and almost significant reduction of the average grain size.

- (2) With the addition level of Sb element to A356, it can be modifiers to the A356 alloy by altered the morphology of the eutectic silicon from coarse acicular to lamellar or fibrous shape. Most of the silicon particles were transformed to rod shape with blunted tips, and rounded shape. Acicular silicon phase was completely absent and lamellar type structure turned to fully modified structure
- (3) The refinement and modification mechanism of A356 is due to the synergistic effect of Sb additions. Antimony combines with aluminium to form AlSb. On further cooling, eutectic reaction takes place, resulting in  $\alpha$ -Al and Si. Probably, these eutectic silicon needles are modified by enhanced nucleation by AlSb substrates available in the liquid. Since each grain of  $\alpha$ -Al forms from one single nucleus, as great the number of nuclei, as more grains will form, thus their size will reduce. If the number of nuclei is sufficiently high, dendritic structures can be avoided as they will have no space to grow, and globular grains of primary  $\alpha$ -Al will preferentially form.

## 7. REFERENCES

- Annual Book of ASM Standard. 2005. Metallographic, Vol 9, pp. 620-630
- Bian X., Wang W., Qin J., 2001, Liquid Structure of Al $\pm$ 12.5% Si Alloy Modified by Antimony, Materials Characterization 46, pp. 25- 29
- Brandes E.A., Brooke G.B. (Eds.). 1998, Smithells Light Metals Handbook, Butterworth- Heinemann, OX, pp. 5-9, 117
- Hao D., Siming X., Jie L., Yu W., Lu L., and Wenbin Y., 2020. Modification of Mg<sub>2</sub>Si Phase Morphology in Mg-4Si Alloy by Sb and Nd Additions. Journal of Materials Engineering and Performance, p 231
- Jiana X., Meeka T.T., Hanb Q., 2006. Refinement of Eutectic Silicon Phase of Aluminium A356 alloy Using High-Intensity Ultrasonic Vibration, Scrip Materialia 54, pp. 893–896.
- Jiana X., Xua H. , Meeka T.T., Hanb Q., 2005. Effect of Power Ultrasound on Solidification of Aluminium A356 alloy, Materials Letters 59, pp. 190– 193.
- Karakosea E., Keskin M., 2009. Effect of Solidification Rate on the Microstructure and Micro Hardness of a Melt Spun Al–8Si–1Sb alloy. Journal of Alloys and Compounds 479 230–236.
- Kazuhiro N., Arne K., 2001. Eutectic Growth pp. 205-216
- KHAN S., ELLIOTT R., 1994, Effect of Antimony on the Growth of Kinetics of Aluminium-Silicon eutectic Alloys, journal of materials science, pp. 736 – 741.
- Mode in Strontium, Antimony and Phosphorus Modified Hypoeutectic Al-Si Foundry Alloys. Materials Transactions, Vol. 42, No, 3 PP. 393 to 396.
- Muhammad S. U., 2Laminu S. K., and Abdulmumin A. A., 2024. Influence of Sodium Chloride Modifier on the Properties of Aluminium-Silicon Alloy Jmme, Vol.14.
- Nataša N., Pavel K., Jan S., Tuong N. V., 2018. Influence of Ca, Sb and Heat Treatment on AlSi9CuMnNi alloy in Frame of their Properties from view of Machining. Matec Web of Conferences 244, 02003.
- Polmear., I.J., 2006. Light Alloys from Traditional Alloys to Nanocrystals, Fourth Edition Melbourne, Australia,
- Qiyang L. 1998, Effect of Antimony on the Growth Kinetics of High purity Al-Si Alloys, Scripta Materialia, Vol. 38, No. 7, pp. 1083–1089

Peng T., Jinshu L., Yixue Y., and Wanyao H., 2023. Microstructure and Mechanical Properties of Cast Al-15Mg2Si-8Si-Based alloy with Various Cr-Sb Ratio Addition, *Journal of Materials Engineering and Performance* p 773.

Prasada Rao A.K., Das K., Murty B.S., . Chakraborty M, 2008, On the Modification and Segregation Behavior of Sb in Al-7Si Alloy During Solidification, *Materials Letters* 62, pp. 2013–2016.

Puga H., Costaa S., Barbosa J., Ribeiro S., ProkicM., 2011. Influence of Ultrasonic Melt Treatment on Microstructure and Mechanical Properties of AlSi<sub>9</sub>Cu<sub>3</sub> alloy, *Journal of Materials Processing Technology*,

Waly M. A. and Reif W., 1993, Thermal Analytical Son the Modification of Al- 7% Si with Addition of Sr & Na, 6<sup>th</sup> Arab International Aluminium Conference- ARAB AL 93, Cairo, 11-14, Dec.

Uzun O., Yilmaz F., Kolemen U., Bas N, 2011, Sb Effect on Micro Structural and Mechanical Properties of Rapidly Solidified Al-12Si alloy, *Journal of Alloys and Compounds* 509, pp. 21–26.

Yu-Chou T., Cheng-Yu C., Sheng-L. L., Chih-K. L., Jing-C L., S.W. Limc, 2009. Effect of Trace La Addition on the Microstructures and Mechanical Properties of A356 (Al-7Si-0.35Mg) aluminum alloys, *Journal of Alloys and Compounds* 487, p. 157–162

Zhu M., Yang G., Yao L., Cheng S, and Zhou Y , 2009. Influence of Al-Ti-B Addition on the Microstructure and Mechanical Properties of A356 alloys. *State Key Rare Metals Vol. 28, No. 2, Apr 2009, p. 181*

Zhongtao Z., Jie L., Hongyun Y., Jian Z., Tingju L., 2009. Microstructure Evolution of A356 Alloy Under Compound Field, *Journal of Alloys and Compounds* 484, pp. 458–46